I-V characteristics of 2D arrays of ultrasmall normal tunnel junctions

1993 J. Phys.: Condens. Matter 5 8375

(http://iopscience.iop.org/0953-8984/5/44/024)

J. Phys.: Condens. Matter 5 (1993) 8375–8390. Printed in the UK

I–V characteristics of 2D arrays of ultrasmall normal tunnel junctions

Sung Jong Lee

The James Franck Institute and Department of Physics, The University of Chicago, 5640 South Ellis Avenue, Chicago, IL 60637, USA

Received 8 June 1993

Abstract. This paper presents simulation results on the dynamics of 2D arrays of ultrasmall normal tunnel junctions at finite temperature, focusing on the possible Kosterlitz–Thouless–Berezinskii transition of charge unbinding. In the case of an array with zero self-capacitance, we find a reasonable agreement between simulation results and the theory. We perform finite-size scaling analysis for linear and non-linear conductances. We also study the effects of self-capacitance and random fractional offset charges, which may be relevant to the experimental situation. In both cases, linear conductances show activated behaviour. A random charge distribution with relatively strong disorder could explain the experimental values of the activation barrier energies.

1. Introduction

Recent developments in micro-fabrication technology have made it possible to observe the so called Coulomb blockade effect in normal or superconducting junctions with cross sections of the order of $(1\ \mu\text{m})^2$ or less, at temperatures of the order of 1 K, provided that the Coulomb charging energy $\sim e^2/2C$ due to the tunnelling of a single electron is bigger than the thermal or quantum fluctuation energy [1]. These conditions can be represented respectively as

$$k_B T \ll e^2/2C \qquad h/R_T C \ll e^2/2C \tag{1.1}$$

where e denotes the charge of an electron and R_T and C are the tunnel resistance and capacitance of a single junction respectively. We see that the second condition requires that the tunnel resistance be much larger than the quantum resistance $R_Q \equiv h/e^2$.

Averin and Likharev [2] developed a semiclassical theory of single-electron tunnelling using a density matrix approach. The main result is that, for a single junction in the current driven situation and in the limit of large resistance R_T, we can describe the tunnelling processes of electrons by the following stochastic tunnelling rate, which depends only on the energy difference of the system before and after tunnelling of an electron. That is,

$$\Gamma = [I(\Delta E/e)/e]\{1 - \exp[-\Delta E/k_B T]\}^{-1} \tag{1.2}$$

where Γ is the tunnelling rate and ΔE is the energy difference of the system before and after tunnelling. $I(V)$ denotes the I–V relation for a voltage driven single junction, which can be represented by an ohmic relation, $I(V) = V/R_T$. Extension of this formula to the case of arrays of junctions under general driving conditions has been made. It has been

0953-8984/93/448375+16$07.50

argued that the so called global rule of tunnelling applies where we can obtain the rate of tunnelling of an electron through a specific junction in the array by substituting for ΔE in the above formula the energy difference (corresponding to the electrostatic equilibrium) of the whole array of junctions after a tunnelling event [3–5]. Monte Carlo simulation of the dynamics of junction arrays can be performed in a staightforward way based on the tunnelling rate for each junction of the array [6].

The state of the array can be represented by the charge configuration with an integer mutiple of the electron charge at each inner metallic island together with some external (e.g. voltage or current) driving conditions. If the array is assumed to be uniform, the interaction energy between two charges in 2D reduces to a screened logarithmic form in the continuum limit, with the screening length proportional to the inverse of the square root of the self-capacitance of the metal islands. This is a Coulomb gas system, with its dynamical law given by the stochastic tunnelling rates. In the 2D Coulomb gas with unscreened interactions, we expect a Kosterlitz–Thouless–Berezinskii transition (hereafter will be referred to as a KTB transition) due to charge unbinding at a finite temperature T_c [7–13].

In this paper, we present some results of Monte Carlo simulations on the dynamics of 2D square arrays of normal tunnel junctions under voltage driven situations. We compare these simulation results with the predictions of KTB transition theory. In the limit of zero self-capacitance, I–V relations show features that are reasonably consistent with the theory. At the transition temperature T_c, we show finite-size scaling of linear and non-linear conductances. Simulations on systems with finite self-capacitance show appreciable deviation from KTB behaviour. In this case, we find activated behaviour of the linear conductance.

Random charges trapped in the substrate layer or junction barrier can induce fractional offset charges on the metal islands [9]. We assumed a Gaussian distribution of offset charges and investigated the I–V relations as the charge disorder is varied. Here, appreciable distortion of the I–V relations, especially suppression of non-linearities, from those of arrays with no disorder is seen. The linear conductance shows activated behaviour with the barrier energy decreasing as the charge disorder increases. Activated behaviour in linear conductance has also been seen in experimental data [12, 14]. It is shown from simulation results that relatively strong charge disorder can explain the experimental results of the activation barrier energies.

2. KTB transition in 2D normal junction arrays

Consider the potential distribution in a 2D square array of normal capacitively coupled junctions (see figure 1) due to a charge distribution. If we denote the charge and the potential on island (i, j) as $Q_{i,j}$ and $\phi_{i,j}$ respectively, we have

$$Q_{i,j} = C[\phi_{i,j} - \phi_{i,j+1}] + C[\phi_{i,j} - \phi_{i+1,j}] + C[\phi_{i,j} - \phi_{i,j-1}] + C[\phi_{i,j} - \phi_{i-1,j}] + C_g\phi_{i,j}. \tag{2.1}$$

Here, C and C_g are the junction capacitance and the self-capacitance to the ground respectively. In typical experimental situations, C is of the order of $\sim 10^{-15}$ F while C_g ranges from 10^{-17} to 10^{-18} F. For $r \gg r_0$ (r_0 is the lattice spacing) we obtain a continuum limit equation for the potential

$$-\nabla^2\phi_0(r) + (1/\lambda_c^2)\phi_0(r) = \rho(r)/C \tag{2.2}$$

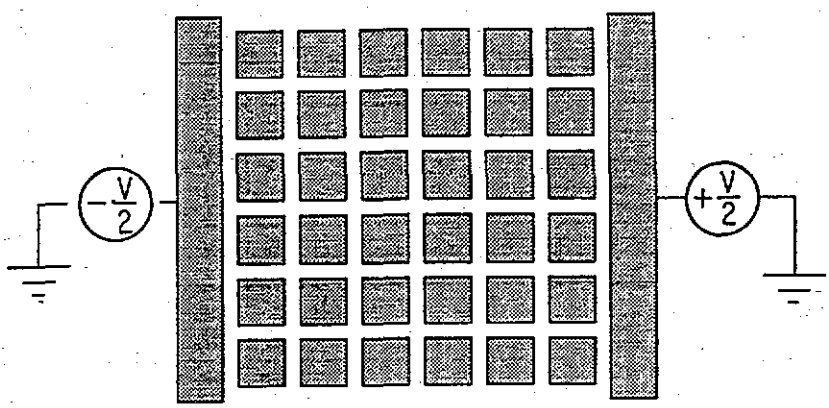

Figure 1. A schematic configuration of a 2D normal junction array. Each island (shaded squares) is coupled capacitively (as well as forming tunnel junctions) with its four nearest neighbours through a uniform junction capacitance C, and also to the ground through self-capacitance C_g. Each tunnel junction is assumed to have a uniform tunnel resistance R_T. A busbar configuration is used for voltage driving.

with $\lambda_c \equiv r_0\sqrt{C/C_g}$ denoting the bare screening length and $\rho(r)$ a suitably normalized charge density from $Q_{i,j}$.

For a sufficiently large bare screening length, the interaction energy between two charges $+e$ and $-e$ separated by r goes as

$$E(r) \simeq \left(e^2/2\pi C\right)\ln\left(r/r_0\right) + 2\mu \tag{2.3}$$

where 2μ denotes the energy needed to produce a pair separated by r_0. Here, we have a realization of a Coulomb gas system. At low temperatures, charge pairs are bound together due to the logarithmic potential of attraction, but at a critical temperature T_c, which is determined by the relation [7]

$$k_B T_c = \left[1/4\pi\epsilon(T_c)\right]e^2/2C \tag{2.4}$$

pairs begin to unbind due to thermal fluctuations. Here, $\epsilon(T_c)$ denotes the dielectric constant at the critical temperature. The dielectric constant is such that $\epsilon(T \to 0) = 1$. Given the value of the chemical potential μ, the dielectric constant at T close to T_c can be calculated by integrating the Kosterlitz RG equation [8]. For infinite square arrays in the limit of vanishing self capacitance (i.e., $\lambda_c = \infty$), μ can be calculated (neglecting the negligible entropic term) to be $\mu = 0.25e^2/2C$ (see appendix B for details). Using the Kosterlitz equation, we obtain $k_B T_c \simeq 0.068E_c$ ($E_c \equiv e^2/2C$) which compares very well with simulation results of $0.067E_c$ determined as the temperature where the I–V power exponent becomes equal to three (see below).

We can relate the dielectric constant to the I–V relation power exponent $a(T)$ defined through $I \simeq V^{a(T)}$ [15, 16]. For a Coulomb gas system under a uniform external electric field $\mathcal{E}$, we can estimate the critical size r_c of a pair of unit charges such that the pair can be broken free. In the case of normal junction arrays, we define the electric field as the average voltage per junction (i.e., one lattice spacing r_0 is the unit of distance). For simplicity of notation, we shall assume that the voltage is measured in units of e/C, energy in units of $E_c \equiv e^2/2C$ and the temperature T in units of E_c/k_B when not explicitly specified.

Then we obtain $r_c/r_0 \simeq 1/2\pi\mathcal{E}$. This means that the energy corresponding to a pair with separation r_c directed parallel to the field $\mathcal{E}$ becomes (we put $E_c \equiv 1$ here)

$$2\mu_{\text{eff}} \simeq (1/\pi\epsilon)\ln(r_c/r_0) + \text{constant} \simeq -(1/\pi\epsilon)\ln(2\pi\mathcal{E}) + \text{constant} \tag{2.5}$$

where the constant term is independent of $\mathcal{E}$ or r_c. Since the current I is proportional to the density n_F of free charges and to $\mathcal{E}$, we obtain

$$I \simeq n_F\mathcal{E} \simeq \exp(-\mu_{\text{eff}}/T)\mathcal{E} \simeq \mathcal{E}^{1/2\pi\epsilon T+1}. \tag{2.6}$$

Since the field $\mathcal{E}$ is proportional to the overall voltage V, we arrive at $a(T) = 1 + 1/2\pi\epsilon T$. Combining this with the condition for T_c, and using the fact that $a(T) = 1$ for $T > T_c$, we can see that $a(T)$ jumps from three to one as T passes T_c from below.

3. Simulation results for $C_g = 0$

The simulation method employed was based on the algorithm by Bakhvalov *et al* [6]. By manipulating the formula for the energy difference, we can update the potential distribution and calculate the energy difference for trial tunnellings without performing mutiplication of the inverse capacitance matrix and the charge configuration vector. In this way, the computing time for one Monte Carlo step is made linearly proportional to the number of sites. Arrays of sizes up to 30×30 were used in simulations with a busbar configuration for voltage driving (figure 1). Periodic boundary conditions were applied along the transverse direction. The number of Monte Carlo tunnelling steps ranged from 2×10^5 to 10^6 depending on the value of the driving voltage. Since the natural time scale for the system is $R_T C$, we measure the current in units of $e/R_T C$.

Figure 2 shows the I–V relations for a uniform 30×30 junction array with zero self-capacitance at various temperatures. The inset of figure 2 shows the resulting I–V power exponent $a(T)$. We obtain the exponent $a(T) \simeq 3.0$ for $k_B T = 0.067 E_c$. This compares quite well to the prediction of the Kosterlitz equation ($k_B T_c \simeq 0.068 E_c$) as mentioned above. This corresponds to the dielectric constant $\epsilon(T_c) \simeq 1.17$. We see that, at low temperatures, there exists a range of voltages where power law behaviour occurs in I–V relations (up to $V/L \simeq 0.2e/C$). This originates from the fact that the logarithmic form of the inter-charge potential no longer holds for distance shorter than the lattice spacing ($r < r_0$). Using the relation between the applied voltage per junction and the pair breaking size, we can estimate the upper cut-off voltage as $V(r_c = r_0)/L \simeq 0.16e/C$ which is close to the above value obtained from the I–V curves.

On the other hand, the finite size of the array gives a lower cut-off voltage for power law behaviour (for $T \leqslant T_c$) because the size of a pair cannot exceed L. For $L = 30$, we obtain $V_{\text{low}}/L \simeq 0.005e/C$. Below the critical temperature, values of the power law slopes $a(T)$ from simulations agree reasonably well with the prediction of the Kosterlitz equation, although at lower temperatures simulation results are systematically a little higher than the theoretical values (up to about 10% at $T = 0.03E_c/k_B \simeq 0.45T_c$). Above T_c, there is some ambiguity in determining $a(T)$ due to screening. In the limit of arrays with infinite size, we could find the sharp jump in $a(T)$ across T_c by measuring the logarithmic slope at an arbitrarily small voltage. However for a finite array, there is a lower cut-off voltage below which a linear I–V relation is obtained even below T_c because of activation into pairs of size L (L is the array size in the direction of the voltage driving). For $T > T_c$, slopes

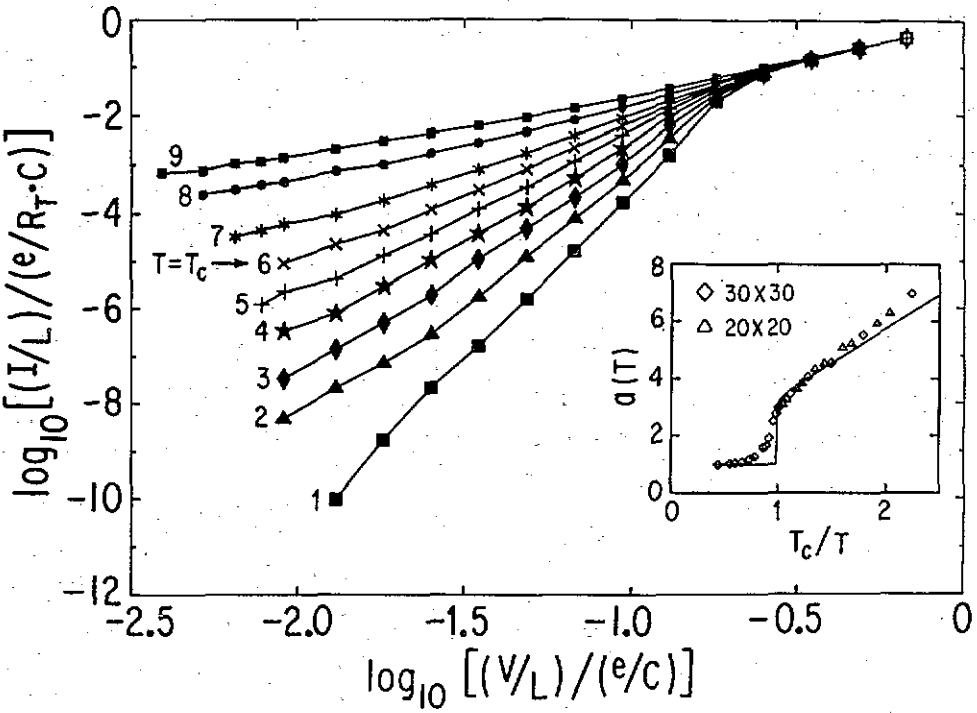

Figure 2. I–V relations for 30×30 array with $C_g = 0$, for temperatures $k_B T/E_c = 0.03$ (1), 0.0375 (2), 0.045 (3), 0.0525 (4), 0.06 (5), 0.067 ($T = T_c$) (6), 0.075 (7), 0.09 (8), and 0.11 (9). The full lines are only guides to the eye. The inset shows I–V power exponents $a(T)$ for different temperatures (for $T \leqslant T_c$ measured at $V/L \simeq 0.04e/C$ and for $T > T_c$ at $V/L \simeq 0.01e/C$) from simulations on a 30×30 array (diamonds), a 20×20 array (triangles) and KTB theory predictions (full line).

measured at applied voltage $V/L \simeq 0.01e/C$ are shown (inset of figure 2). We can see a broadened transition into linear I–V relations.

Next consider the linear conductance of junction arrays with vanishing self-capacitance. In the limit of infinite size of the array, for temperatures below T_c, all charges are bound, thus the linear conductance (which will be denoted by G) vanishes in this case. For $T > T_c$, KTB theory gives the well known square root cusp form for the conductance of an array with width W and length L

$$G = (W/L)G_0 \exp\left[-2b\frac{1}{\sqrt{[(T - T_c)/T_c]}}\right] \tag{3.1}$$

where b is a constant of the order of unity and G_0 is of the order of $\sim 1/R_T$ (R_T is the tunnel resistance of a junction). Indeed our simulation results (from I–V curves of 30×30 arrays) showed a square root cusp form for the linear conductance (these were obtained from an average over three or four values of I/V for applied voltages between $V/L = 0.002e/C$ and $V/L = 0.007e/C$) and we could obtain an estimate of $2b \simeq 2.1$. For comparison, simulations by Bobbert *et al* [13], obtained $2b \simeq 1.8$, which approximately agrees with the present result. This value should not be taken too seriously, because the square root cusp form is valid only for temperatures near T_c, i.e., for $(T - T_c)/T_c \ll 1$ in the limit of

large arrays, while some of our simulation data points lie outside this domain of validity. A theoretical estimate based on our value of the chemical potential μ gives $2b \simeq 4$, which is about twice as large as our simulation results on 30×30 arrays. This discrepancy is probably due to the fact that the size of the array (30×30) is still smaller than the screening length near T_c, and that our simulations overestimate the real (large L-limit) linear conductance in this region.

For a finite-size array, there is a non–vanishing linear conductance even for temperatures below T_c due to thermal activation of charge pairs with the size of the array L (in the direction of the voltage driving). At temperatures below T_c, the energy to create a pair with size L is (again putting $E_c \equiv 1$)

$$2E_L \simeq (1/\pi\epsilon)\ln(L/r_0) + 2\mu \tag{3.2}$$

where 2μ is the chemical potential for creating a pair with the size of a lattice spacing r_0. In the case of a finite-size array with length L (and with an arbitrary width W), these pairs become free and the effective number density of free charges that are created by thermal activation will behave as

$$n_F \simeq \exp(-E_L/T) \simeq (1/L)^{1/2\pi\epsilon T}. \tag{3.3}$$

If we deal with junction arrays with the same width and length ($W = L$), the size dependence of linear conductance of an array will depend on L as

$$G_L \simeq (1/L)^{1/2\pi\epsilon T}. \tag{3.4}$$

Hence, if we define $G_L \simeq L^{-z(T)}$ then we see that $z(T) = 1/2\pi\epsilon T$ for $T \leqslant T_c$ and in particular at $T = T_c$ we obtain $z(T_c) = 2$ from the condition for T_c. Also we expect $a(T) = z(T) + 1$ from (2.6).

Figure 3 shows the size dependence of linear conductance at temperatures below or equal to T_c using the simulation results on small size arrays (of equal width and length). We find a clear power law dependence of the linear conductance on the size of the array below or equal to T_c. Good agreement is found between $z(T) + 1$ and $a(T)$ near T_c but $z(T) + 1$ tends to be larger than $a(T)$ at lower temperatures (see the inset of figure 3).

Now let us consider the size dependence of the non-linear I–V relations at the transition temperature T_c [17]. At T_c, the correlation length is infinite and hence, for a finite size array, the only relevant length scale is the size L of the array. Suppose that an external electric field $\mathcal{E}$ is applied to the array. Then the typical scale of free energy change due to the coupling of the system to the external field is $e\mathcal{E}L$. This corresponds to the thermal fluctuation energy $k_B T_c$ when $\mathcal{E}$ is equal to $\mathcal{E}_t$ with

$$\mathcal{E}_t = k_B T_c / eL. \tag{3.5}$$

If we hypothesize finite-size scaling for the I–V relation, i.e., that the current density J is a homogeneous function of $\mathcal{E}$ and L^{-1} (or $\mathcal{E}_t$), then we obtain the following *ansatz* form of the I–V relation:

$$J \simeq \mathcal{E}L^{-z(T_c)} f(e\mathcal{E}L/k_B T_c) \tag{3.6}$$

where f is the scaling function and $z(T_c) = 2$ from KTB theory. We can see that $f(x) \to$ constant as $x \to 0$ in order to match the finite-size scaling behaviour of the linear conductance at T_c, and in the limit of large L, we recover the relation $I \simeq V^{1+z(T_c)} = V^3$.

Figure 4 shows a finite-size scaling plot of I–V relations at $T = T_c$ for $L \times L$ arrays with $L = 3, 4, 5, 7, 9$, where we find a good collapse of the I–V relations with a choice of the parameter $z(T_c) = 2.0$ that agrees very well with the KTB theory.

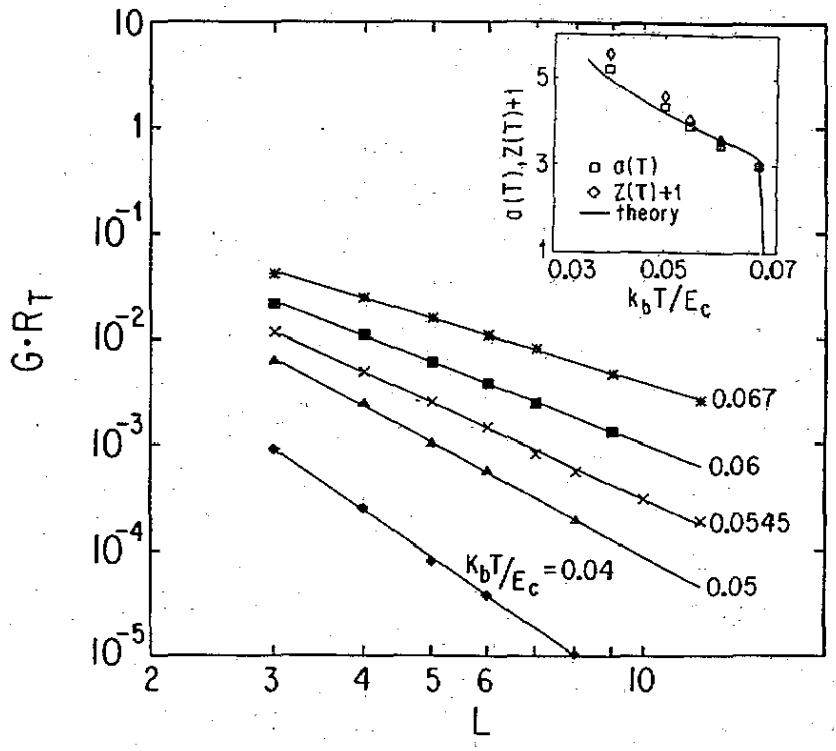

Figure 3. Size dependence of linear conductances for $T \leqslant T_c$; $k_BT = 0.04E_c$ (diamonds), $k_BT = 0.05E_c$ (triangles), $k_BT = 0.0545E_c$ (crosses), $k_BT = 0.06E_c$ (squares), and $k_BT = 0.067E_c$ (stars). The inset shows a comparison between $z(T) + 1$ (diamonds, see the text for definition) and $\alpha(T)$ (squares) from measurements of I–V power exponents, as well as the KTB theory result for $\alpha(T)$ (full curve).

4. Effect of self-capacitance and random offset charges

There always exists some finite self-capacitance C_g in the array in real experimental situations due to the capacitive coupling between the metallic islands and the ground plane. This will give a bare screening length $\lambda_c = r_0\sqrt{C/C_g}$ which approximately sets the limit of the length scale where logarithmic interaction is valid. In the rigorous sense, there is no phase transition in the case of an array with finite C_g, even though some features of broadened transition might remain if $C_g \ll C$.

Figure 5(a) shows the I–V curves of 20×20 arrays for the case of self-capacitance $C_g = 0.01C$. In this case, the bare screening length is $\lambda_c = 10r_0$, which is smaller than the array size. Due to this finite bare screening, even at low temperature, the I–V relations do not show features of well defined power law slopes, even though there exists an appreciable portion of the range of the applied voltages where the slope can be determined quite precisely. Figure 5(b) shows the corresponding I–V power exponent $\alpha(T)$ for $C_g = 0.01C$ evaluated at two different scales of the applied voltage, one at $V/L \simeq 0.01e/C$ and the other at $V/L \simeq 0.04e/C$. The latter gives approximately the maximum power law slope. We can see that there exists an appreciable dependence of the power law slopes on the scale of the applied voltage and that these slopes show some suppression from the results of KTB theory. As C_g increases, this suppression was found

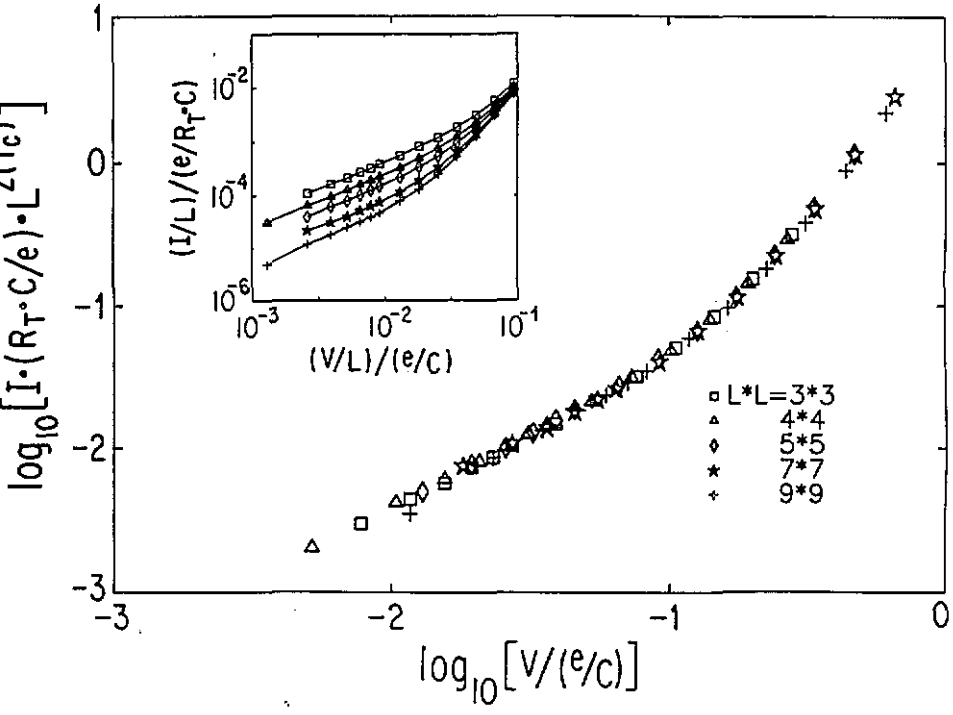

Figure 4. Scaling plot of non-linear conductance (I–V relation) at T_c for arrays with sizes $L \times L$ ($L = 3, 4, 5, 7, 9$). The inset shows the raw data for I–V relations.

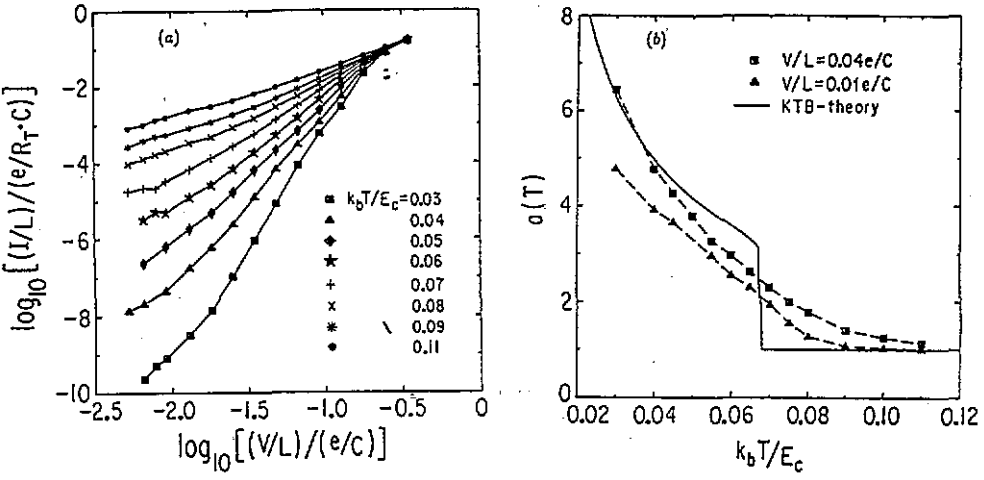

Figure 5. (*a*) I–V relations for $C_g = 0.01C$ for temperatures ranging from $T = 0.03E_c/k_B$ to $T = 0.11E_c/k_B$. The full lines are only guides to the eye. (*b*) I–V power exponent $\alpha(T)$ versus temperature for $C_g = 0.01C$ with slopes measured at $V/L \simeq 0.04e/C$ (squares) and $V/L \simeq 0.01e/C$ (triangles). The full curve shows the KTB theory.

to be bigger. In particular, near the temperature at which the pure KTB system ($C_g = 0$)

undergoes a KTB transition, $a(T)$ shows a rather featureless broadening without passing through the value $a(T) = 3$.

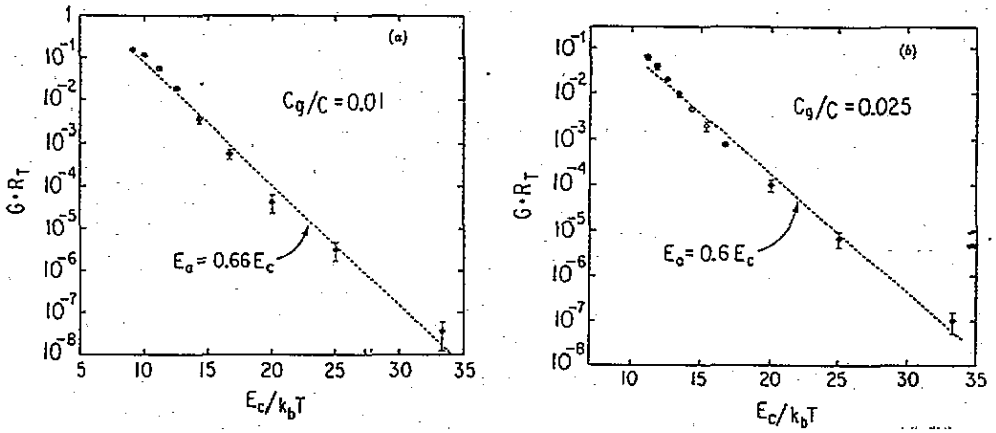

Figure 6. (*a*) Linear conductance versus inverse temperature of a 20×20 array for $C_g = 0.01C$. The broken line is an activation fit with $E_a \simeq 0.66E_c$. (*b*) Linear conductance versus inverse temperature of a 24×24 array for $C_g = 0.025C$. The broken line is an activation fit with $E_a \simeq 0.6E_c$.

Figure 6 shows the linear conductance versus temperature. We can see an approximately activated behaviour with activation barrier energies $E_a(C_g = 0.01C) \simeq 0.66E_c$ and $E_a(C_g = 0.025C) \simeq 0.6E_c$. These values can be interpreted roughly as the energy (per particle) needed to create a pair of charges with the size of the screening length. If we denote this by E_p, then we obtain $2E_p \simeq (E_c/\pi\epsilon_{eff}) \ln(\lambda_c/r_0) + 2\mu$, with ϵ_{eff} the effective dielectric constant and λ_c the screening length. By putting $\epsilon_{eff} \simeq 1$ (at low temperature), we obtain $E_p(C_g = 0.01C) \simeq 0.62E_c$ and $E_p(C_g = 0.025C) \simeq 0.54E_c$. These values are fairly close to the values of activation barrier energies given above.

The size dependence of conductance (for $L \times L$ arrays with $L = 3, 4, \cdots, 20$) is shown in figure 7 at temperature $T = 0.03E_c/k_B$ for three values of the self-capacitance, $C_g = 0.11C$, $0.025C$, and $0.01C$. These correspond to bare screening lengths of $\lambda_c \simeq 3r_0$, $6r_0$, and $10r_0$ respectively. We can see that the power law dependence of the conductance on array size ceases to hold near the scale of the bare screening length. Eventually the conductivity will turn into a constant plateau at large L. The inset of figure 7 shows an attempt to fit these size dependence of the linear conductance into a scaling form of $G(L) = L^{-z}g(L/\lambda_c)$ with a choice of $z = 5.6$. We can see only a rough scaling behaviour. This may be attributable partly to the fact that we used the bare screening length λ_c as the scaling parameter, while more accurate treatment should use the effective screening length (due to the finite-temperature effect), which is not easy to estimate.

Mooij *et al* [9] pointed out the existence of random fractional offset charges induced on islands due to, for example, trapped charges in the substrate layer or the dielectric tunnel barrier of the array of islands. If we imagine that a trapped charge polarizes both the metal island and the ground electrode, then the junction area will have some fractional charges induced due to the polarization. We can model the system by simply assuming that there exist some (quenched) random fractional charges on metallic islands. This is a dual analogue of Josephson junction arrays under random magnetic frustration as dealt with by

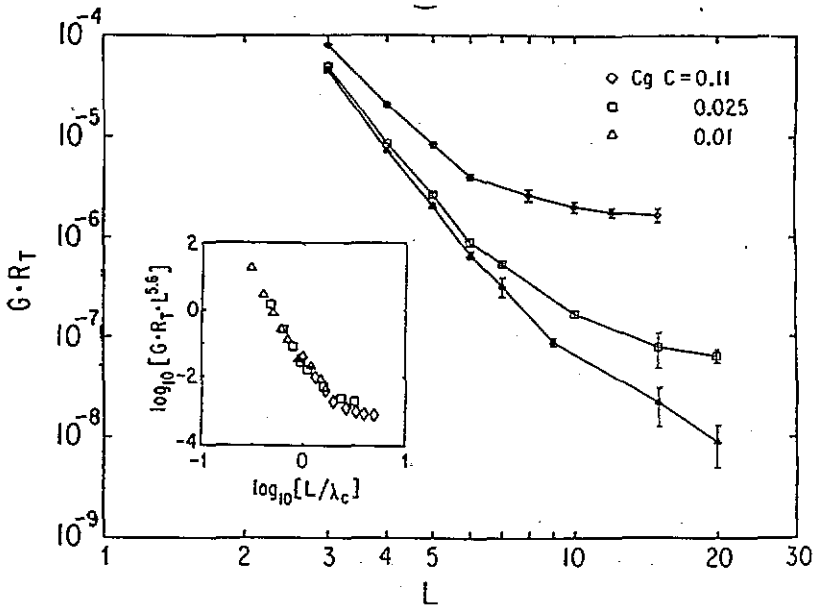

Figure 7. Size dependence of the linear conductance at $T = 0.03E_c/k_B$ for $C_g = 0.11C$ (diamonds), 0.025C (squares), and 0.01C (triangles) respectively. The full lines are only guides to the eye.

Granato and Kosterlitz [18]. They showed that the KTB transition is destroyed by this kind of disorder.

Suppose now that the distribution of random charge on each island has a Gaussian distribution with an RMS width of Q_{RMS}, that is $P(q) \propto \exp(-q^2/2Q_{RMS}^2)$ where $P(q)$ denotes the probability density for finding a random fractional charge q on an island. Then, the average net charge within an area d^2 goes as $Q_d \simeq Q_{RMS}\sqrt{N}$ where $N \simeq (d/r_0)^2$ is the number of sites within an area of linear size d. Thus, we obtain

$$Q_d \simeq Q_{RMS} d/r_0. \tag{4.1}$$

Hence the effect of a charge e will be washed out at a distance d_c such that $Q_{RMS}d_c/r_0 = e$ or $d_c = r_0(e/Q_{RMS})$.

Figure 8(a) and (b) shows the I–V relations of 16×16 arrays for $Q_{RMS} = 0.1e$ ($d_c = 10r_0$) and $Q_{RMS} = 0.25e$ ($d_c = 4r_0$) respectively. The self-capacitance is assumed to be zero here. We emphasize that the latter case is rather close to the maximal disordered situation which can be taken as that of random charges distributed uniformly between $-0.5e$ and $+0.5e$. For the case of moderate disorder $Q_{RMS} = 0.1e$, the I–V curves show an interesting feature with the power law slope varying smoothly from linear behaviour into some non-linear one as the applied voltage increases. As the charge disorder is increased to $Q_{RMS} = 0.25e$, the non-linearity of the I–V curves is suppressed significantly. Typical power law slopes extracted from around $V/L \simeq 0.04e/C$ are shown in figure 8(c) for both cases of the charge disorder, where we can confirm the trend of the suppression of the I–V non-linearity as the charge disorder increases. Also, this suppression is much more effective than in the case of non-zero C_g only, especially at lower temperatures.

Figure 9(a) shows the linear conductance versus temperature of these arrays as well as a 16×16 array with maximal disorder (as defined above), where we find thermally activated

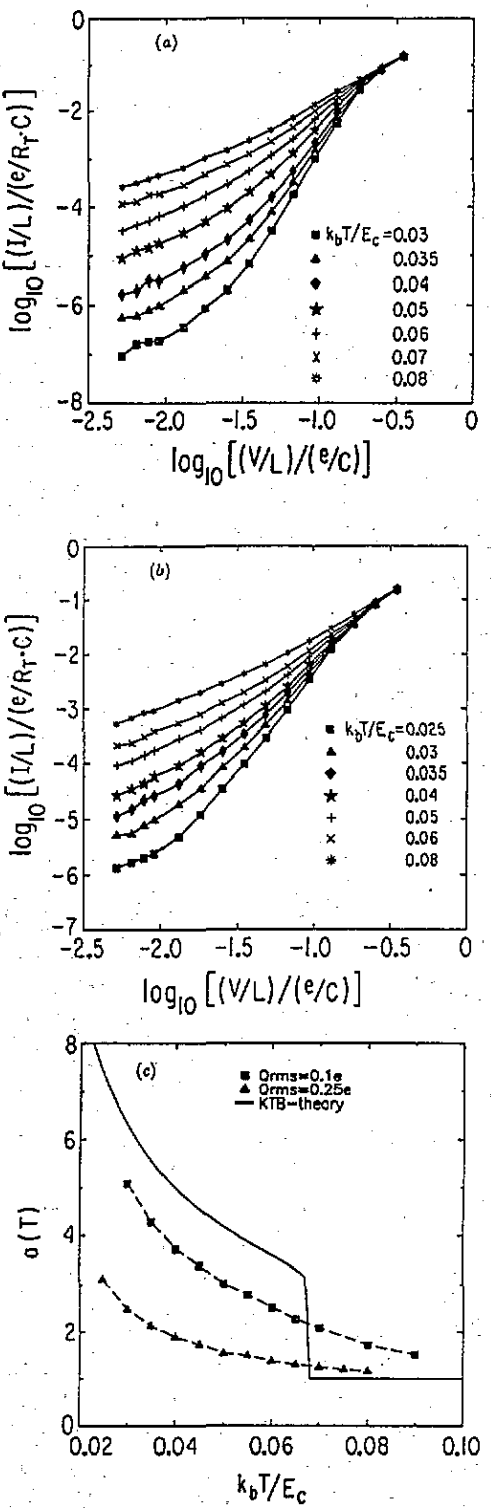

Figure 8. (*a*) *I–V* relations of a 16 × 16 array with random offset charges $Q_{RMS} = 0.1e$. The temperature ranges from $0.03E_c/k_B$ to $0.08E_c/k_B$. The full lines are only guides to the eye. (*b*) *I–V* relations of a 16 × 16 array with random offset charges $Q_{RMS} = 0.25e$. The temperature ranges from $0.025E_c/k_B$ to $0.08E_c/k_B$. The full lines are only guides to the eye. (*c*) $a(T)$ versus temperature from (*a*) and (*b*) measured at $V/L \simeq 0.04e/C$ for $Q_{RMS} = 0.1e$ (squares) and $Q_{RMS} = 0.25e$ (triangles). The full curve shows the KTB theory.

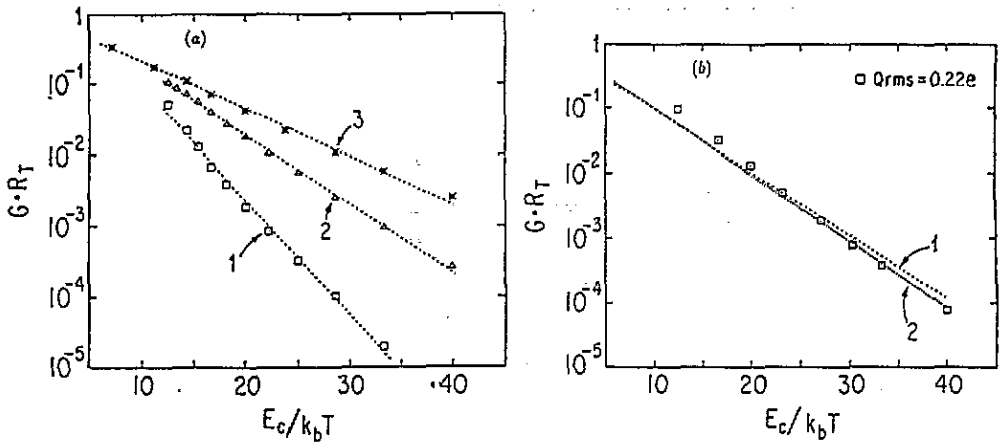

Figure 9. (*a*) Linear conductance versus inverse temperature of a 16×16 array: $Q_{RMS} = 0.1e$ (squares, 1); $Q_{RMS} = 0.25e$ (triangles, 2); maximally disordered array (stars, 3; random charges distributed uniformly between $-0.5e$ and $0.5e$). The numerical errors are about the size of the symbols. The broken lines are activation fits with $E_a \simeq 0.37E_c$ (1), $E_a \simeq 0.22E_c$ (2), and $E_a \simeq 0.16E_c$ (3). (*b*) A comparison between simulation results (squares, linear conductance versus inverse temperature for a 16×16 array with $Q_{RMS} = 0.22e$; the numerical errors are about the size of the symbols) and experimental results (lines) by Tighe *et al* [14] of linear conductance measurements on two samples of 50×70 junction arrays. Shown here are only the activation fits to the experimental data (not the raw data) for two sample arrays with R_T = 38 kΩ, $E_c/k_B = 2.2$ K (1) and R_T = 126 kΩ, $E_c/k_B = 2.5$ K (2) (with permission from Dr T Tighe).

behaviour with activation barrier energies $E_a(Q_{RMS} = 0.1e) \simeq 0.37E_c$, $E_a(Q_{RMS} = 0.25e) \simeq 0.22E_c$, and E_a (maximal disorder) $\simeq 0.16E_c$. Here we note that the activation fit in the case of charge disordered arrays works better than that in the case of finite C_g. We can see that charge disorder is more effective than finite C_g in reducing the activation barrier energy, even though we do not have a quantitative theoretical estimate for the activation energies in case of charge disorder to compare with above simulation results. We also calculated the linear conductance for small size arrays with Gaussian charge disorder. However, we could not obtain a smooth behaviour in the size dependence of the linear conductance due to lack of self-averaging in the case of small arrays with quenched charge disorder.

In one experiment by the Delft group on a sample of a 190×60 array with $C_g < 0.01C$, activated linear conductance with a barrier energy of $E_a \simeq 0.24E_c$ was reported. More recently, Tighe *et al* [14] obtained similar values for a few sample arrays of 50×70 normal tunnel junctions made of aluminum islands. In these experiments, the self-capacitances were a few times $0.001C$ (hence a little less than the $0.01C$ of our simulations). One interesting experimental result is that samples of arrays with different values of junction capacitances ranging by about a factor of four all showed similar values ranging from 0.23 to 0.27 for the ratio E_a/E_c ($E_c = e^2/2C$). These values are much smaller than the $0.66E_c$ that we obtained from our simulations on a 20×20 array with the self-capacitance effect only (using $C_g = 0.01C$). This suggests that an additional effect of random charge disorder would be necessary to explain this suppression of the barrier energy in the experimental results. This can be seen in the above examples of simulations on arrays with random charge disorder, where we obtain a more effective reduction of the activation barrier energy and, in particular, the strongly disordered case of $Q_{RMS} = 0.25e$ gives rise to an activation barrier

energy of $0.22E_c$ that happens to be rather close to the experimental values cited above. Figure 9(*b*) shows a comparison between simulation results (squares, linear conductances of 16×16 arrays with $Q_{RMS} = 0.22e$) and the experimental results of Tighe *et al* cited above. The two lines are activation fits to the linear conductance data (raw data are not shown here) for two samples, rescaled by the tunnel resistances R_T and the charging energies E_c of the two samples. We can see that both samples show approximately the same value (~ 0.23) for the ratio E_a/E_c. Simulation results of the linear conductances for this case of $Q_{RMS} = 0.22e$ agree approximately with the experimental data especially at lower temperatures, even though the activation energy $E_a \simeq 0.26E_c$ from simulations is a little higher than the experimental value of $0.23E_c$.

One possibility to explain the experimental result that the ratio E_a/E_c is approximately constant is that the similar fabrication process of these arrays may induce roughly the same value of charge disorder (Q_{RMS} around $0.22e$–$0.24e$) that corresponds to the observed activation energy. Note that the same value of Q_{RMS} gives rise to the same ratio of E_a/E_c independent of the magnitude of the junction capacitance C. However, more precise determination of the array parameters, especially the junction capacitance would be necessary for obtaining a more reliable magnitude of the charging energy E_c (and hence of E_a/E_c) in the experiments and understanding the physical origin of the activation barrier energies. Also needed are detailed measurements of I–V relations in the non-linear regime (especially at low temperature) that can be compared with simulations in order to put a more stringent test on the relevance of charge disorder in the dynamics of the arrays.

5. Conclusions and discussion

In this paper, we have presented results of Monte Carlo simulations on the dynamics of 2D square arrays of ultrasmall normal tunnel junctions in connection with a possible KTB transition and the effect of self-capacitance or charge disorder. For systems with zero self-capacitance, reasonable agreement is found with KTB theory especially below T_c, including the I–V power exponent $\alpha(T)$ for $T \leqslant T_c$ and finite-size scaling of the non-linear conductance at T_c. However, it appears that the size of the arrays used in simulations (30×30) is not large enough to identify the sharp jump above T_c. Also, even though a square root cusp form of the linear conductance seems to hold approximately, the coefficient $2b$ obtained from simulations turns out to be only about half of a theoretical estimate for infinite arrays.

Finite self-capacitance or random offset charges are shown to induce appreciable deviation from KTB behaviour in the characteristics of I–V curves. In both cases, activated behaviour of the linear conductance is seen. Quantitatively, it would be difficult to compare the simulations with experimental results, because the exact value of the charge disorder is not known for experimental situations and also because there is a certain limitation in the determination of the precise values of the junction capacitances and the tunnel resistances. However, simulation results show that charge disorder is effective in reducing the activation barrier in linear conductance and that a random charge distribution with relatively strong disorder can possibly explain the experimental values of the activation barrier energies. In this regard, the measured values of activation barrier energies in experiments might serve as an indirect measure of the charge disorder for the arrays.

Acknowledgments

This work was supported by the Materials Research Laboratory at the University of Chicago. The author is grateful to Professor T Halsey for support and discussions. The author also wants to thank Dr H Borsje, Professor H Jaeger, Professor K Likharev and Dr T Tighe for discussions. He expresses special thanks to Dr T Tighe for explaining his experiments to him and also for allowing him to use some of his experimental data in this work. Generous help from Professor T Witten for part of the computing time is gratefully acknowledged. This work was presented as a thesis to the Department of Physics of the University of Chicago, in partial fulfillment of the requirements for the PhD degree.

Appendix A. An efficient method for updating the potential distribution and evaluating the trial tunnelling energy

Let us first consider the change of potential distribution when tunnelling from site r_i to site r_f occurs. Using the charge–potential relation equation (2.1), and the fact that only the charge at sites r_i and r_f changes (by a unit charge $\pm e$), we can easily obtain the following relation:

$$\phi'(r) - \phi(r) = e[\tilde{C}^{-1}_{r,r_f} - \tilde{C}^{-1}_{r,r_i}] \tag{A1}$$

where $\phi'(r)$ and $\phi(r)$ denote the potential at site r after and before the tunnelling respectively and $\tilde{C}$ is the capacitance matrix defined through equation (2.1) rewritten in a matrix form. Note that r, r_i, and r_j should be understood as the discrete indices for the sites of metal islands. Equation (A1) holds for the case when both r_i and r_f are inner islands. When edge electrodes are involved, we can simply omit the corresponding (inverse) capacitance matrix element. One can see that the potential can be updated by simply using the (stored) two matrix elements for each site. Hence we do not need to multiply the inverse capacitance matrix by the charge configuration vector at each tunnelling step.

Next, we need a formula for the energy difference for a trial tunnelling from site r_i to r_f. From simple electrostatic considerations, we have

$$\Delta E(r_i \to r_f) = (e/2)[\phi'(r_f) + \phi(r_f) - \phi'(r_i) - \phi(r_i)]. \tag{A2}$$

If we use the previous relation equation (A1), then this becomes

$$\Delta E(r_i \to r_f) = e[\phi(r_f) - \phi(r_i)] + (e^2/2)[\tilde{C}^{-1}_{r_i,r_i} + \tilde{C}^{-1}_{r_f,r_f} - 2\tilde{C}^{-1}_{r_i,r_f}]. \tag{A3}$$

Here again, we see that only the 'old' potential $\phi(r)$ and two elements of the inverse capacitance matrix are needed to calculate ΔE for each trial tunnelling. Hence, at the beginning of each Monte Carlo step, we can prepare the initial potential, and then we can evaluate the transition rates for all trial tunnellings using the energy given by equation (A3).

Appendix B. Chemical potential for creating a pair

Here, we consider an evaluation of the energy cost for creating a pair of charges $+e$ and $-e$ with separation of a unit lattice spacing r_0. We assume that the array consists of a $L \times L$

square lattice of normal metal islands with a periodic boundary condition imposed on both directions for convenience of calculation.

Junction capacitances are uniform and equal to C and each island has a uniform self capacitance C_g to the ground. The charge–potential relation is the same as equation (2.1), and can be concisely written as

$$\tilde{C}\phi = Q \tag{B1}$$

where $\tilde{C}$ abbreviates the capacitance matrix and ϕ and Q are the potential and charge distribution vector, respectively.

An important quantity is the inverse capacitance matrix $\tilde{C}^{-1}$. By using Fourier representation, it is simple to obtain

$$\tilde{C}^{-1}_{r,r'} = \frac{1}{C}\sum_{m,n=0,\cdots,L-1}\frac{1}{L^2}\frac{\exp[i2\pi m(x-x')/L]\exp[i2\pi n(y-y')/L]}{4\sin^2(m\pi/L)+4\sin^2(n\pi/L)+C_g/C}. \tag{B2}$$

Here, (x, y) and (x', y') are the integer cartesian coordinates of r and r' respectively in units of r_0. Using the result of appendix A, the energy needed to create a pair at separation of a unit lattice spacing is

$$2\mu = (e^2/2)\left[2\tilde{C}^{-1}_{0,0} - 2\tilde{C}^{-1}_{0,r_0}\right] \tag{B3}$$

where r_0 denotes a unit lattice vector.

Therefore, using the expression for $\tilde{C}^{-1}$, we obtain in the limit of infinite size of the array ($L \to \infty$),

$$2\mu = \left(\frac{e^2}{2C}\right)^2\int_0^1 dx\int_0^1 dy\frac{1-\cos(2\pi x)}{4\sin^2(\pi x)+4\sin^2(\pi y)+C_g/C}. \tag{B4}$$

In the limit of $C_g \to 0$, we obtain

$$\mu = \tfrac{1}{4}(e^2/2C). \tag{B5}$$

In general, we can express μ in terms of elliptic integrals as follows:

$$\mu = \begin{cases} \frac{1}{4}(e^2/2C)\left[1-(C_g/2\pi C)K\left(\sqrt{1-C_g/2C}\right)\right] & C_g/2C < 1 \\ \frac{1}{4}(e^2/2C)\left[1-(1/2\pi)\sqrt{2C_g/C}\,K\left(\sqrt{1-2C/C_g}\right)\right] & C_g/2C > 1 \end{cases} \tag{B6}$$

where $K(x)$ denotes the complete elliptic integral of the first kind.

References

[1] Averin D V and Likharev K K 1991 *Mesoscopic Phenomena in Solids* ed B L Altshuler, P A Lee and R A Webb (Amsterdam: Elsevier)

[2] Averin D V and Likharev K K 1986 *J. Low Temp. Phys.* **62** 345

[3] Nazarov Yu V 1989 *Sov. Phys.–JETP* **68** 561

[4] Ingold G L and Nazarov Yu V 1992 *Single Charge Tunneling (NATO ASI Series)* ed H Grabert and M H Devoret (New York: Plenum)

[5] Grabert H, Ingold G L, Devoret M H, Estève D, Pothier H and Urbina C 1991 *Z. Phys.* **B84** 143

[6] Bakhvalov N S, Kazacha G S, Likharev K K and Serdyukova S I 1989 *Sov. Phys.–JETP* **68** 581; 1990 *Physica* B **165 & 166** 963
[7] Kosterlitz J M and Thouless D J 1973 *J. Phys. C: Solid State Phys.* **6** 1181
[8] Kosterlitz J M 1974 *J. Phys. C: Solid State Phys.* **7** 1046
[9] Mooij J E, van Wees B J, Geerligs L J, Peters M, Fazio R and Schön G 1990 *Phys. Rev. Lett.* **65** 645
[10] Geerligs L J, Anderegg V F and Mooij J E 1990 *Physica* B **165 & 166** 973
[11] Fazio R and Schön G 1990 *Physica* B **165&166** 1127
[12] Peters M 1990 *PhD Thesis* Delft University of Technology
[13] Bobbert P A, Geigenmüller U, Fazio R and Schön G 1991 *Macroscopic Quantum Phenomena* ed T D Clark, H Prance, R J Prance and T P Spiller (Singapore: World Scientific)
[14] Tighe T S, Tuominen M T, Hergenrother J M and Tinkham M 1993 *Phys. Rev.* B **47** 1145
[15] Ambegaokar V, Halperin B I, Nelson D R and Siggia E D 1980 *Phys. Rev.* B **21** 1806
[16] Minnhagen P 1987 *Rev. Mod. Phys.* **59** 1001
[17] Fisher D, Fisher M P A and Huse D A 1991 *Phys. Rev.* B **43** 130
[18] Granato E and Kosterlitz J M 1986 *Phys. Rev.* B **33** 6533